

# Induction Coil Sensors – a Review

Slawomir Tumanski, *Member, IEEE*

**Abstract** – The induction coil sensors (called also search coils, pickup coils or magnetic loop sensors) are described. The design methods of air coils and ferromagnetic core coils are compared and summarized. The frequency properties of the coil sensors are analyzed and various methods of output signal processing are presented. Special kinds of induction sensors, as Rogowski coil, gradiometer sensors, vibrating coil sensors, tangential field sensors and needle probes are described. The application of coil sensor as magnetic antenna is presented.

**Index Terms** – coil sensor, magnetic field measurement, search coil, Rogowski coil, vibrating coil, gradiometer, integrator circuit, H-coil sensor, needle probe method.

## I. INTRODUCTION

The induction coil sensor [1,2] (called also search coil sensor, pickup coil sensor, magnetic antenna) is one of the oldest and well-known magnetic sensors. Its transfer function  $V = f(B)$  results from the fundamental Faraday's law of induction

$$V = -n \cdot \frac{d\Phi}{dt} = -n \cdot A \cdot \frac{dB}{dt} = -\mu_0 \cdot n \cdot A \cdot \frac{dH}{dt} \quad (1)$$

where  $\Phi$  is the magnetic flux passing through a coil with an area  $A$  and a number of turns  $n$ .



Fig.1. The simplest sensor of magnetic field in form of a coil

The operating principle of the coil sensor is generally known, yet the details and know-how are known only for specialists. For example, it is a common knowledge that the output signal,  $V$ , of a coil sensor depends on the rate of change of flux density,  $dB/dt$ , therefore the application of integration is necessary. Nonetheless, there are other useful methods, which enable obtaining results proportional to flux density,  $B$ . Again, it is widely known that in order to improve the sensitivity the coil should have large number of turns and large active area. However, the optimization process of the coil performance is not so obvious in many cases.

The coil sensor was described in detail many years ago [3]. However, today still the sensors based on the same operating principle are widely used in many applications. For instance, nowadays the awareness of large stray magnetic fields potentially dangerous increased significantly. The induction sensor is practically the only sensor, which can be feasibly manufactured directly by its users (in contrary to Hall-, magnetoresistive- or fluxgate-type sensors). The technology of manufacturing is simple, the materials (winding wire) are commonly available. Thus, everyone can perform such investigations using a simple and low-cost (yet accurate) induction coil sensor.

There are more examples of the renaissance of various coil sensors. The Chattock-Rogowski coil was first described in nineteenth century, in 1887 [4,5]. Today, in twenty first century, this sensor is re-discovered as excellent current transducer [6] and sensor used in measurements of magnetic properties of soft magnetic materials [7]. The old Austrian patent from 1957 [9] describing the use of needle sensor (called also stylus or probe) for investigation of local flux density in electrical steel was rediscovered several years ago [10,11].

The main goal of this paper is to summarize the existing knowledge about induction coil sensors, including old, often forgotten publications, as well as new developments. It is organized as follows: two main designs of coils sensor (air coil and core coil) are described. Then, their frequency response is analyzed taking into account sensors and output electronics. Next, special kinds of induction sensors are discussed and followed by description of the most popular application of the inductive sensor – magnetic antenna. Finally, main advantages and drawbacks of this sensor are discussed.

## 2. AIR COILS VERSUS FERROMAGNETIC CORE COILS

The relatively low sensitivity of an air coil sensor and problems with its miniaturization can be partially overcome by incorporation of a ferromagnetic core, which acts as a flux concentrator, inside the coil. For coil with a ferromagnetic core the, equation (1) can be rewritten as

$$V = -\mu_0 \cdot \mu_r \cdot n \cdot A \cdot \frac{dH}{dt} \quad (2)$$

For the reason that modern soft magnetic materials exhibit relative permeability,  $\mu_r$ , even larger than  $10^5$  this can result in a significant increase of the sensor sensitivity. However, it should be taken into account that resultant permeability of the core,  $\mu_c$ , can much lower than the material permeability due to the demagnetizing field effect expressed by the geometry dependent demagnetizing factor  $N$

$$\mu_c = \frac{\mu_r}{1 + N \cdot (\mu_r - 1)} \quad (3)$$

If the permeability of material  $\mu_r$  is relatively large (which is generally the case) the resultant permeability of the core  $\mu_c$  depends mainly on the demagnetizing factor  $N$ . Thus, for high permeability material the sensitivity of the sensor depends mostly on the dimensions and geometry of the core.

The demagnetizing factor  $N$  for an ellipsoidal shape of the core depends on the core length  $l_c$  and core diameter  $D_c$  according to an approximate equation

$$N \cong \frac{D_c^2}{l_c^2} \cdot \left( \ln \frac{2l_c}{D_c} - 1 \right) \quad (4)$$

It can be derived from equation (4) that in order to obtain small value of  $N$  (and large resultant permeability  $\mu_c$ ) the core should be long and with small diameter. Let us consider the dimensions of the search coil sensor optimized for a large sensitivity as described in [12]. The core was prepared from amorphous ribbon (Metglas 2714AF) with dimensions  $l_c = 300$  mm and  $D_c = 10$  mm (aspect ratio equal to 30). Substituting these values into equation (4) we obtain  $N \cong 3.5 \cdot 10^{-3}$  what

means that the sensitivity is about 300 times larger in comparison with the air coil sensor.

Therefore, the application of a core made of soft magnetic material leads to significant improvement of the sensor sensitivity. However, this enhancement is obtained with a sacrifice of one of the most important advantages of the air coil sensor – linearity. The core made even from the best ferromagnetic material introduces to the transfer function of the sensor some non-linear factors depending on temperature, frequency, flux density, etc. Additional magnetic noise (e.g. Barkhausen noise) also decreases the resolution of the sensor. And what can be very important, the ferromagnetic core disturbs the investigated magnetic field (or flux density).

### 3. DESIGN OF THE AIR COIL SENSOR

A typical design of an air coil sensor is presented in Fig.2. The resultant area of a multilayer coil sensor can be determined by performing an integration [3]

$$A = \frac{\pi}{4} \cdot \frac{1}{D - D_i} \cdot \int_{D_i}^D (y^2) dy = \frac{\pi}{12} \cdot \frac{D^3 - D_i^3}{D - D_i} \quad (5)$$

Relation (5) is of limited accuracy, therefore in practice it is better to determine the resultant area of the coil experimentally – by means of calibration in a known field. For the sake of straightforwardness for further analysis of the sensitivity in this paper, the area is determined by using a simplified formula obtained by assumption that the diameter of the coil is equal to mean value  $D_m = (D + D_i)/2$ , thus

$$A = \frac{\pi}{8} \cdot (D + D_i)^2 \quad (6)$$

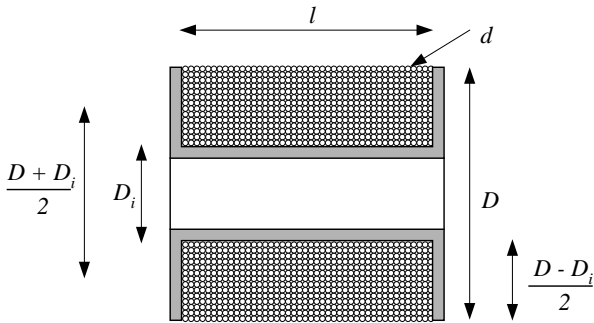


Fig.2. Typical design of an air coil sensor ( $l$  – length of the coil,  $D$  – diameter of the coil,  $D_i$  – internal diameter of the coil,  $d$  – diameter of the wire)

If we assume that flux density to be measured is a sine wave  $b = B_m \cdot \sin(\omega t)$ , and the sensing coil is a ring with diameter  $D$ , the relation (1) can be rewritten in a form

$$V = 0.5 \cdot \pi^2 \cdot f \cdot n \cdot D^2 \cdot B \quad (7)$$

where  $f$  is a frequency of the measured field,  $n$  and  $D$  are number of turns and diameter of the coil, respectively.  $B$  is the measured flux density.

If we would like to determine the magnetic field strength  $H$  instead of flux density  $B$ , then the dependence (7) can be easily transformed knowing that for non-ferromagnetic medium  $B = \mu_0 \cdot H$  ( $\mu_0 = 4 \cdot \pi \cdot 10^{-7}$  H/m) and

$$V = 2 \cdot 10^{-7} \cdot \pi^3 \cdot f \cdot n \cdot D^2 \cdot H \quad (8)$$

Taking into account (6) the equation (8) can be presented as

$$V = \frac{10^{-7}}{2} \cdot \pi^3 \cdot f \cdot n \cdot (D + D_i)^2 \cdot H \quad (9)$$

The number of turns depends on the diameter  $d$ , of used wire, on the packing factor  $k$  ( $k \approx 0.85$  [1]) and on dimensions of the coil

$$n = \frac{l \cdot (D - D_i)}{2 \cdot k \cdot d^2} \quad (10)$$

Thus, the sensitivity  $S = V/H$  of an air coil sensor can be calculated as

$$S = \frac{10^{-7}}{4} \cdot \frac{\pi^3 \cdot f \cdot l}{k d^2} \cdot (D - D_i) \cdot (D + D_i)^2 \quad (11)$$

The resolution of the coil sensor is limited by thermal noise. This noise  $V_T$  depends on the resistance  $R$  of the coil, the temperature  $T$ , the frequency bandwidth  $\Delta f$  with coefficient equal to the Boltzman factor  $k_B = 1.38 \cdot 10^{-23}$  W·s/K

$$V_T = 2 \sqrt{k_B \cdot T \cdot \Delta f \cdot R} \quad (12)$$

The resistance of the coil can be determined as [13]

$$R = \frac{\rho \cdot l}{d^4} \cdot (D - D_i) \cdot (D + D_i) \quad (13)$$

and the signal-to-noise ratio,  $SNR$ , of the air coil sensor is

$$SNR = \frac{\pi^3 \cdot 10^{-7}}{8} \cdot \frac{f}{\sqrt{\Delta f}} \cdot \frac{\sqrt{l} \cdot (D + D_i) \cdot \sqrt{D^2 - D_i^2} \cdot H}{\sqrt{k^2 \cdot k_B \cdot T \cdot \rho}} \quad (14)$$

As can be seen from equation (14) the sensitivity increases roughly proportionally to  $D^3$  and  $SNR$  increases with  $D^2$  the best way to obtain maximal sensitivity and resolution is to increase the coil diameter  $D$ . Less effective is the increase of the coil length, because the sensitivity increases with  $l$ , while the  $SNR$  increases only with  $\sqrt{l}$ . The sensitivity can also be increased by the increase of the number of turns. For example, by using wire with smaller diameter – sensitivity increases with  $d^2$  and  $SNR$  ratio does not depend on the wire diameter.

Various publications discussed other geometrical factors of the air coil sensor. For instance, the optimum relation between the length and the diameter of the coil can be determined taking into account the error caused by inhomogeneous field. It was found [3,14] that for  $l/D = 0.866$  the undesirable components are eliminated at the center of the coil. This analysis was performed for the coil with one layer. For a multilayer coil this recommended relation is  $l/D = 0.67 - 0.866$  (0.67 for  $D_i/D = 0$  and 0.866 for  $D_i/D = 1$ ). The same source [3] recommends  $D_i/D$  to be less than 0.3.

It can be concluded from the analysis presented above that in order to obtain high sensitivity the air coil sensor should be very large. For instance, the induction coil magnetometer used for measurements of micropulsations of the Earth's magnetic field in the bandwidth 0.001-10 Hz with resolution 1 pT – 1 nT [15] have meter-range dimensions and even hundreds of kilogram weight. An example of a design of the coil sensor for such purpose was presented in [16]. The coil with diameter 2 m (16 000 turns of copper wire 0.125 mm in diameter) detected micropulsation of flux density in the bandwidth 0.004 - 10

Hz. For 1 pT field the output signal was about - 0.32  $\mu\text{V}$ , whilst thermal noise level was about 0.1  $\mu\text{V}$ .

The air coil sensor with 10 000 turns and diameter 1 m was used to detect flux density of magnetic field in  $\text{pT}$  range (for magnetocardiograms) [17].

Coil sensors are sensitive only to the flux that is perpendicular to their apertures. Therefore, in order to determine all directional components of the magnetic field vector, three mutually perpendicular coils should be used (Fig. 3). An example of such a low-noise three-axis search coil magnetometer is described in [18]. The “portable” magnetometer consists of three coils with diameters 19-33 cm, number of turns 4100 - 6500 and weight 14 kg and is capable of measuring the magnetic field in bandwidth 20 Hz - 20 kHz with noise level lower than 170 dB/100  $\mu\text{T}$ .

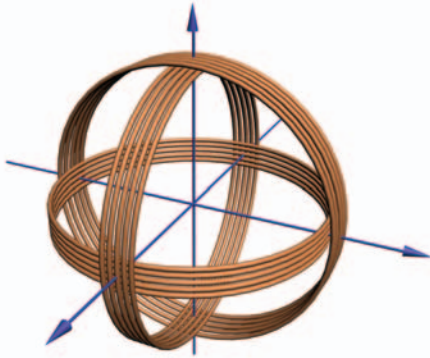


Fig.3. The concept of three mutually perpendicular coils for three-axis magnetic field measurements

On the other hand, there are examples of extremely small air-cored sensors. Three orthogonal coil system with dimensions less than 2 mm and weight about 1 mg (40 turns) was used for detection of position of small, fast moving animals [19].

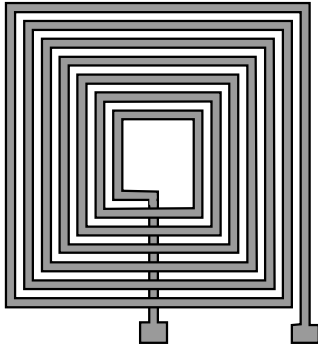


Fig. 4. An example of a pickup planar thin film coil designed for eddy-current sensors [20]

The air-coil sensors are widely used as eddy-current proximity sensors or eddy-current sensors used for non-destructive testing (e.g. for detection of cracks). In such a case the sensitivity is not as important as the spatial resolution and compactness of the whole device. Such sensors are often manufactured as a flat planar coil (made in PCB or thin film technology [20-24]) connected to an on-chip CMOS electronic circuit [21]. An example of such a sensor with dimensions  $400 \times 400 \mu\text{m}$  (7 turns) is presented in Fig. 4.

Sometimes, the frequency response of the air-core sensor is more important factor is than the sensitivity or spatial resolution. The dimensions of the coil can be optimized for better frequency performance. These factors are discussed later.

#### 4. DESIGN OF FERROMAGNETIC CORE COIL SENSOR

The high-permeability core coil sensors are often used in the case when large sensitivity or dimension limitations are important. A typical geometry of such a sensor is presented in Fig.5.

The optimal value of core diameter  $D_i$  was determined as  $D_i \cong 0.3 D$  [13]. The length of the coil  $l$  is recommended to be about 0.7-0.9  $l_c$ . For such coil dimensions the output signal  $V$  and  $SNR$  ratio at room temperature can be described as [25]

$$V \cong 0.9 \cdot 10^{-5} \cdot f \cdot \frac{l^3}{d^2} \cdot D_i \cdot \frac{1}{\ln(2 \cdot l / D_i) - 1} \cdot H \quad (15)$$

$$SNR \cong 1.4 \cdot 10^8 \cdot \frac{f}{\sqrt{\Delta f}} \cdot l^2 \cdot \sqrt{l} \cdot \frac{1}{\ln(2 \cdot l / D_i) - 1} H \quad (16)$$

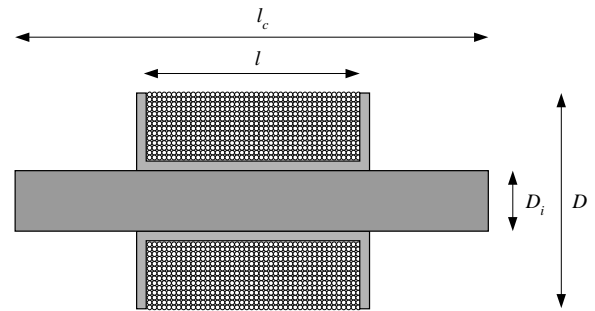


Fig.5. Design of a typical ferromagnetic core coil sensor ( $l$  – length of the coil,  $l_c$  – length of the core,  $D$  – diameter of the coil,  $D_i$  – diameter of the core)

From the relationships (15) and (16) it can be concluded that in the case of coil sensor with ferromagnetic core the most efficient method of improving of the sensor performance is to make the length of the core (or rather the ratio  $l/D_i$ ) as large as possible (the sensitivity is proportional to  $l^3$ ). Figure 6 presents the dependence of the resultant permeability of the core  $\mu_c$  on the aspect ratio  $l/D$  and the core material permeability  $\mu_r$  determined in [13].

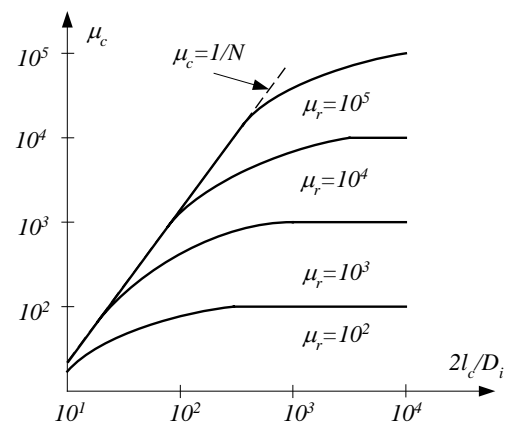


Fig.6. The dependence of the resultant permeability of the core on the dimensions of the core and the permeability of the material [13]

The choice of the aspect ratio of the core is very important. The length should be sufficiently large to profit from the permeability of the core material. On the other hand, if the aspect ratio is large the resultant permeability depends on the material permeability, which

may cause error resulting from the changes of material permeability due to the temperature or frequency. For large values of material permeability the resultant permeability  $\mu_c$  practically does not depend on material characteristic because relation (3) is then

$$\mu_c \approx \frac{1}{N} \quad (17)$$

A higher value of material permeability allows using longer core without a risk that the resultant permeability depends on material magnetic features.

As an example, let us consider a low-noise induction magnetometer described in [26]. The core was prepared from temperature independent amorphous ribbon (Metglas 2714AF) with dimensions: length 150 mm, cross section around  $5 \times 5$  mm (aspect ratio of around 27). A coil of 10 000 turns was wound with 0.15 mm diameter wire. The noise characteristic of this sensor is presented in Fig. 7. The obtained noise level around 0.05 pT/ $\sqrt{\text{Hz}}$  was comparable with the values reported for SQUID sensors.

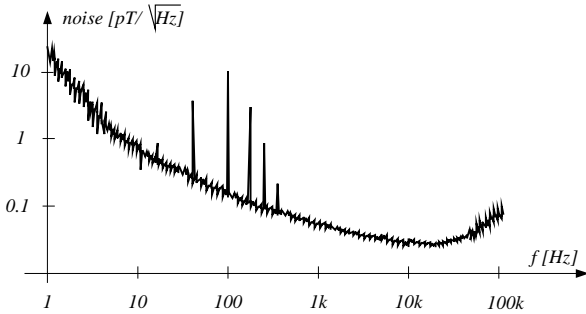


Fig. 7. An example of the noise performance of the induction magnetometer (after [26])

The same authors compared the influence of the core material – for an amorphous Metglas core the noise was at the level of 0.05 pT/ $\sqrt{\text{Hz}}$ , whilst the same sensor with a permalloy Supermumetal core exhibited larger noise – at the level of 2 pT/ $\sqrt{\text{Hz}}$ . Also, the comparison of air coil and ferromagnetic core sensors has been reported [27,28]. Experimental results show that correctly designed ferromagnetic core induction sensors exhibited linearity comparable with the air core sensors.

Sensors with ferromagnetic core are often used for magnetic investigations in space research [29,30]. Devices with the length of core 51 cm and the weight 75 g (including preamplifier) exhibited the resolution (noise level) 2 fT/ $\sqrt{\text{Hz}}$  [31]. In analysis of the space around the Earth (OGO Search coil experiments) the following three-axis sensors have been used: coil 100 000 turns of 0.036 mm in diameter, core made from nickel-iron alloy 27 cm long and square ( $0.6 \times 0.6$  cm) cross-section. Each sensor weighted 150 g (a half of the weight was the core weight). The sensitivity was 10  $\mu\text{V/nT Hz}$  [32].

There are commercially available search coil sensors. For example, MEDA offers sensors with sensitivity 25 mV/nT and noise at 10 kHz equal to 10 fT/ $\sqrt{\text{Hz}}$  (MGCH-2 sensor with core length about 32 cm) or at 0.2 Hz equal to 25 pT/ $\sqrt{\text{Hz}}$  (MGCH-3 sensor with core length of about 1 m) [33].

## 5. FREQUENCY RESPONSE OF SEARCH COIL SENSORS

Considering the relationship (1) it is obvious that in order to obtain the output voltage signal of the sensor the flux density must be varying in time. Therefore, the coil sensors are capable of measuring only the AC magnetic fields. In the case of the DC magnetic fields the variation of the flux density can be “forced” in the sensors by moving the coil.

However, the term “DC magnetic field” can be understood as a relative one. By using a sensitive amplifier and a large coil sensor it is possible to determine the magnetic fields starting from frequency of several mHz [15,16]. Thus, it is also possible to investigate the quasi-constant magnetic fields with stationary, unmovable coil sensor.

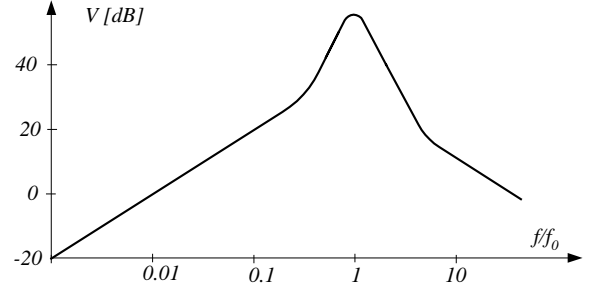


Fig.8. Typical frequency characteristic of an induction coil sensor

Typically using coil sensors the AC magnetic fields with frequency up to several MHz can be investigated. In special design this bandwidth can be extended to GHz range [34,35]. An example of typical frequency characteristic of a coil sensor is presented in Fig. 8.

According to (7) the output signal depends linearly on frequency, but due to the internal resistance  $R$ , inductance  $L$  and self-capacitance  $C$  of the sensor the dependency  $V = f(f)$  is more complex. The equivalent electric circuit of the induction sensor is presented in Fig. 9.

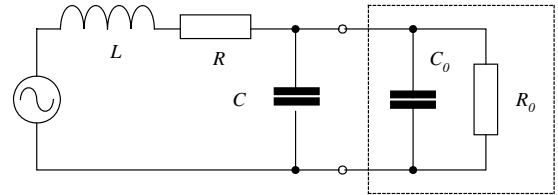


Fig. 9. Equivalent circuit of induction sensor loaded with capacity  $C_0$  and resistance  $R_0$

The output signal increases, initially almost linearly, with the frequency of measured field, up to resonance frequency

$$f_0 = \frac{1}{2 \cdot \pi \cdot \sqrt{L \cdot C}} \quad (18)$$

Above the resonance frequency the influence of self-capacitance causes the output signal to drop.

Analyzing the equivalent circuit of the sensor, the sensitivity  $S=V/H$  can be presented in a form [36]

$$S = \frac{S_0}{\sqrt{(1+\alpha)^2 + \left(\beta^2 + \frac{\alpha^2}{\beta^2} - 2\right) \cdot \gamma^2 + \gamma^4}} \quad (19)$$

where:  $\alpha = R/R_0$ ,  $\beta = R \cdot \sqrt{C/L}$ ,  $\gamma = f/f_0 = 2 \cdot \pi \cdot f \cdot \sqrt{L \cdot C}$

The absolute sensitivity  $S_0$  can be described as  $S_0 = 2 \cdot 10^{-7} \cdot \pi^3 \cdot n \cdot D^2$ . The graphical form of the relation (19) is presented in Fig. 10.

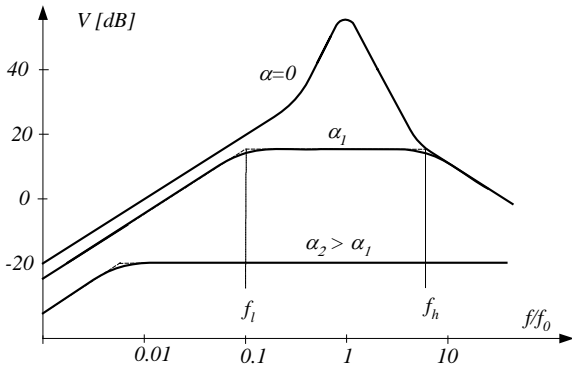


Fig. 10. Frequency characteristics of the induction coil loaded by the resistance  $R_0$  (the coefficient  $\alpha = R/R_0$ )

The sensor loaded with a small resistance  $R_0$  exhibits frequency characteristic with a plateau between the low corner frequency

$$f_l = \frac{R + R_0}{2 \cdot \pi \cdot L} \quad (20)$$

and the high corner frequency

$$f_h = \frac{1}{2 \cdot \pi \cdot R_0 \cdot C} \quad (21)$$

Frequently used method of improvement of the sensor frequency characteristic is the connection of a load with very low resistance to the sensor output (current to voltage converter). By appropriate choice of the ratio  $R/L$  it is possible to alter the low frequency corner of the bandwidth.

The inductance of the sensor depends on the number of turns, permeability and the core dimensions according to the following empirical formula [36]

$$L = n^2 \cdot \frac{\mu_0 \cdot \mu_c \cdot A_c}{l_c} \cdot \left( \frac{l}{l_c} \right)^{-3/5} \quad (22)$$

The self-capacitance of the sensor strongly depends on the construction of the coil (for example application of an external shield and the shield between the coil layers significantly changes the capacity).

The frequency characteristic below the  $f_l$  can be additionally improved by incorporation of the PI correction circuit (more details are given in the next section).

A feedback circuit is another method of improvement of the frequency characteristic of the sensor [37,38] as presented in Fig.11.

The output signal of the circuit presented in Fig. 11 can be described as [37]

$$V_{out} = 2 \cdot \pi \cdot f \cdot n \cdot \mu_0 \cdot \mu_c \cdot A_c \cdot \frac{R_F}{2 \cdot \pi \cdot M} \cdot \frac{j \cdot \omega / \omega_l}{1 + j \cdot \omega / \omega_l} \cdot \frac{1}{1 + j \cdot \omega / \omega_h} \cdot B_x \quad (23)$$

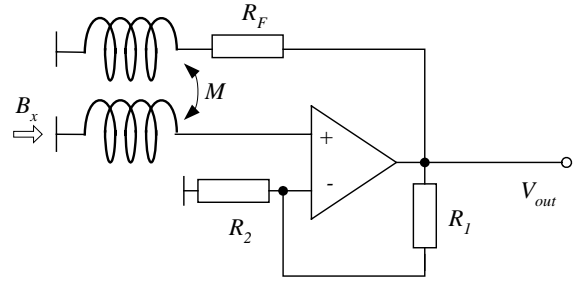


Fig.11. Induction coil sensor connected to the amplifier with negative transformer type feedback

The circuit described by equations (23) represents a high-pass filter working under condition  $\omega \ll \omega_b$ , and a low-pass filter for  $\omega \gg \omega_b$ . As a result, the frequency characteristic is flat between low frequency

$$\omega_l = \frac{R_F}{M} \cdot \frac{1}{1 + R_1 / R_2} \quad (24)$$

and high frequency

$$\omega_h = \frac{1 + R_1 / R_2}{R_F} \cdot M \cdot \omega_0 \quad (25)$$

The air core sensors, due to their relatively low inductance, are used as the large frequency bandwidth current transducer (in Rogowski coil configuration described later) typically up to 1 MHz with an output integrator and up to 100 MHz with current to voltage output - in so called "self integration" mode.

## 6. ELECTRONIC CIRCUITS CONNECTED TO THE COIL SENSORS

Because the output signal of an induction coil is dependent on the derivative of the measured value ( $dB/dt$  or  $dI/dt$  in the case of Rogowski coil) one of the methods of recovering the original signal is by means of an integrating transducer [39] (Fig.12).

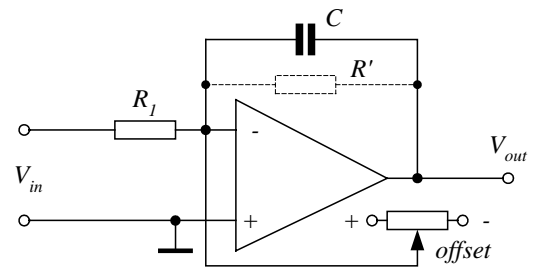


Fig.12. Typical integrating circuit for the coil signal

Fig. 12 presents a typical analogue integrating circuit. The presence of the offset voltage and associated zero drift are a significant problem in correct design of such transducers. For this reason, an additional potentiometer is sometimes used for offset correction and resistor  $R'$  is introduced for the limitation of the low frequency bandwidth. The output signal of integrating transducer is

$$V_{out} = -\frac{1}{R \cdot C} \cdot \int_{t_0}^{T+t_0} (V_{in}) dt + V_0 \quad (26)$$

where  $R=R_1+R_{coil}$ . The resistance  $R$  should be sufficiently large (as not to load the coil) as well as the capacitance  $C$ . - typical values are  $R_1 = 10\text{ k}\Omega$  and  $C = 10\text{ }\mu\text{F}$  [39].

The amplifier can introduce several limitations in the high-frequency bandwidth. A passive integrating circuit (Fig.13) exhibits somewhat better performance in this bandwidth. Combinations of various methods of integration (active and passive) can be used for large bandwidth- as proposed in [49].

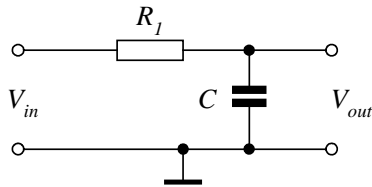


Fig. 13. The passive integrating circuit

Problems with correct designing of a measuring system with integrating transducer are often overcome by applying low resistance loading of the coils (self-integration mode presented in Fig. 10). Usually, a current-to-voltage converter is used as an output transducer, sometimes additionally supported by a low-frequency correction circuit. An example of such a transducer is presented in Fig. 14.

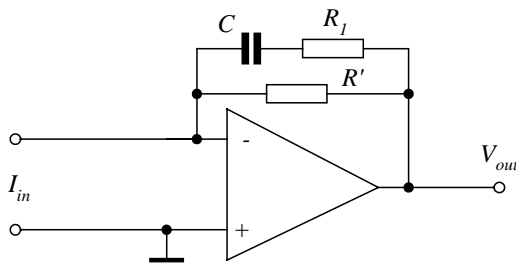


Fig.14. Current to voltage transducer with additional frequency correction circuit. An example described in [26] with elements:  $R_1 = 100\text{ k}\Omega$ ,  $C = 0.22\text{ }\mu\text{F}$ ,  $R' = 47\text{ M}\Omega$ .

In the current-to-voltage transducer presented in Fig. 14 the correction circuit  $R_1C$  is introduced to correct the characteristic of low-resistance loaded circuit at lower frequencies – as it is illustrated in Fig. 15.

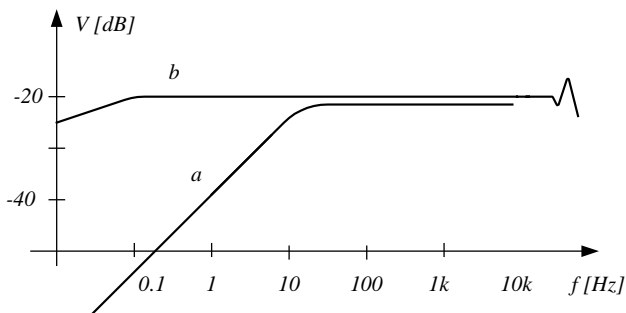


Fig. 15. Frequency characteristic of a coil sensor with current-to-voltage transducer (a) and with additional correction circuit (b)

The above-described circuits were equipped with analogue transducers at the output of the coil sensor. However, it is also possible to convert the output signal to a digital form and then to perform

digital integration – several examples of such approaches (with satisfying results) have been described in [41-43].

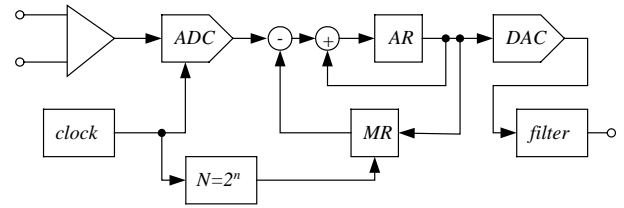


Fig.16. Digital transducer of the coil sensor signal (after [43])

Accurate digital integration of the coil sensor signal it is not a trivial task. Also, in digital processing there are integration zero drifts. The most frequently used method eliminating this problem is the subtraction of the calculated average value of the signal. The integrating period, sampling frequency and triggering time should be carefully chosen, especially when the exact frequency of the processed signal is unknown. Moreover, cost of a good quality data acquisition circuit (analogue-to-digital converter) is relatively high and a use of a PC is necessary. Therefore, in some cases the integrating process is performed digitally by relatively simple hardware (without a PC), consisting of analogue-to-digital (ADC) and digital to analogue (DAC) circuits and registers (AR and MR in Fig. 16).

It is worth noting that almost all companies manufacturing the equipment for magnetic measurements (as Brockhaus, LakeShore, Magnet Physik, Walker Scientific) offer digital integrator instruments, called Fluxmeters – often equipped with the coil sensors. Fig. 17 presents the coil sensor used in this instrument.

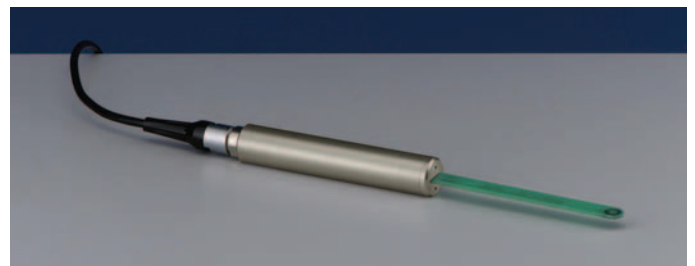


Fig.17. An example of the coil sensor used in a digital fluxmeter of Brockhaus

The amplifier connected to the coil sensor introduces additional noise – voltage noise and current noise, as it is illustrated in Fig. 18. Each noise component is frequency dependent. Analysis of the coil sensor connected to the amplifier [1] indicates that for low frequency the thermal noise of the sensor dominates. Above the resonance frequency the amplifier noise dominates.

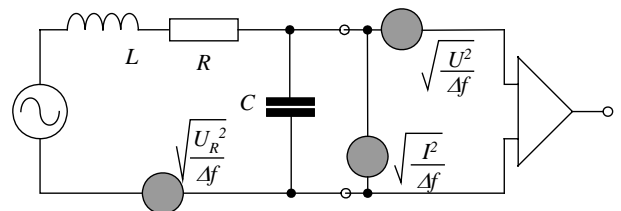


Fig. 18. The sources of the noise in the equivalent circuit of the coil connected to amplifier

The reduction of the amplifier noise can be achieved by application of a HTS SQUID picovoltmeter, as it has been reported in [44]. Indeed, the noise level of the preamplifier was decreased to a level of

110 pV/√Hz, but the dynamic performances of such a circuit were deteriorated.

## 7. SPECIAL KINDS OF INDUCTION COIL SENSORS

### 7.1. The moving coil sensors

One of the drawbacks of the induction coil sensor – sensitivity only to varying magnetic fields can be overcome by moving the coil. For example, if the coil is rotating (Fig.19) with quartz-stabilized rotational speed it is possible to measure DC magnetic fields with very good accuracy. The main condition of the Faraday's law (the variation of the flux) is fulfilled, because the sensor area varies as  $a(t) = A \cdot \cos(\omega t)$  and the induced voltage is

$$V = -B_x \cdot n \cdot A \cdot \sin(\omega \cdot t) \quad (27)$$



Fig. 19. The sensor of a DC magnetic field with a rotating coil

Instead of rotation it is possible to move the sensor in another ways, and the most popular method is the use of a vibrating coil. One of the first such ideas was applied by Groszkowski, who in 1937 demonstrated the moving coil magnetometer [45]. The coil was forced to vibrate by connecting it to a rotating eccentric wheel.

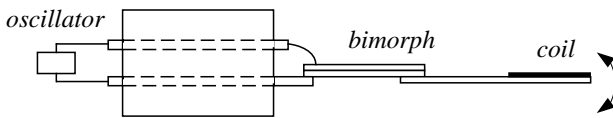


Fig.20. The vibrating cantilever magnetic field sensor (after [47])

One of the best excitation methods of the vibrating coil is by connecting it with a vibrating element, as for example piezoelectric ceramic plate [46,47]. Due to relatively high frequency of vibration (in the kHz range) it is possible to make very small sensor with good geometrical resolution. Fig. 20 presents an example of a pickup coil sensor mounted to a piezoelectric bimorph cantilever. The ten-turn coil 30 μm wide and 0.8 μm thick excited to a vibration frequency of around 2 kHz (mechanical resonance frequency) exhibited the sensitivity of around 18 μV/100 μT [47].

It is also possible to perform measurements by quick removal of the coil sensor from the magnetic field (or quick insertion into the magnetic field). Such extraction coil method (with application of digital fluxmeter with large time constant) enables measuring DC magnetic field according to the following relationship [48]

$$\int V dt = -n \cdot A \cdot (B_x - B_o) \quad (28)$$

The moving coil methods are currently rather rarely used, because generally it is tendency to avoid any moving parts in the measuring instruments. For measurements of DC magnetic field Hall sensors and fluxgate sensors are most frequently used.

### 7.2. The gradiometer sensors

The gradiometer sensors (gradient sensors) are commonly used in SQUID magnetometers for elimination of the influence of ambient field. These sensors can be also used in other applications where the ambient field disturbs the measurements, or determination of the magnetic field gradient itself [49].

The operating principle of the gradiometer sensor is presented in Fig. 21. The external magnetic field is generated by a large and distant source (for example Earth's magnetic field), so we can assume that this field is uniform. If two coil sensors (with small distance between them) are inserted in such a field then both will sense the same magnetic field. Because both coils are connected differentially (see Fig. 21) the influence of the external field is eliminated. If at the same time near both of the coils there is a smaller source of magnetic field (for example human heart investigated for magnetocardiogram) the magnetic field in the coil placed nearer the source is larger than in the other coil. This small difference (the gradient of magnetic field) is therefore detected by the gradiometer sensor. In this way it is possible to measure relatively small magnetic field from a local source in the presence of much larger magnetic field from a distanced one.

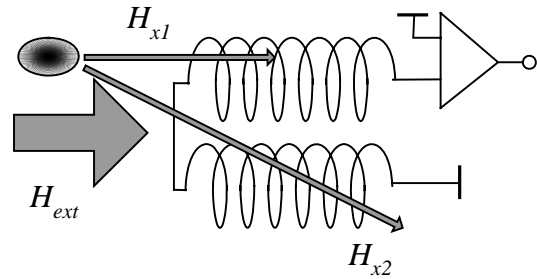


Fig. 21. Operating principle of gradiometer sensor

Fig. 22 presents typical arrangements of the gradiometer coils: vertical, planar and asymmetric. A correctly designed gradiometer coil should indicate zero output signal when inserted into uniform field. In the asymmetric arrangement the sensing coil is smaller and must have more turns in order to compensate the magnetic field detected by the larger coil.

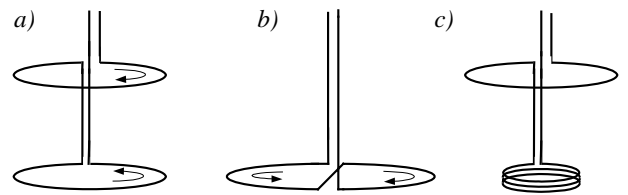


Fig.22. Gradiometer coils arranged: a) vertically, b) horizontally, c) asymmetrically

It is possible to improve the ability to reject the common component by employing several gradiometers. Fig. 23 presents a first order, second order (consisting of two gradiometers of a first order) and third-order gradiometers.

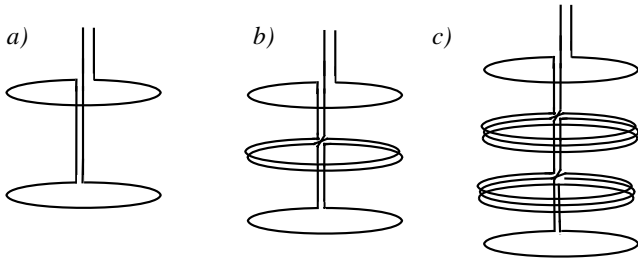


Fig. 23. Gradiometers of a) first-order, b) second-order, c) third-order

Fig. 24 presents a typical response of the gradiometer coils to the source distant from the sensor [50]. The first order gradiometer rejects more than 99% of the source distanced by  $300b$  ( $b$  is the distance between the single coils of the gradiometer). For the second order gradiometer this distance is diminished to about  $30b$ . It is possible to arrange even higher order of the gradiometer (Fig. 23c presents the gradiometer of the third-order), but this results in a reduced sensitivity and SNR ratio.

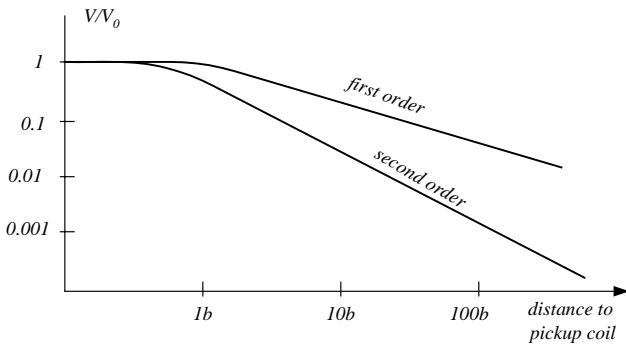


Fig. 24. A typical response of a gradient coil sensor to the source distanced from the pickup coil – relative to response for the source with distance smaller than  $0.3b$  ( $b$  the distance between coils of gradiometer) (after [50])

The quality of the gradiometer sensor is often described by the formula

$$V \propto G + \beta \cdot H \quad (29)$$

where  $G$  is the gradient of the measured field and  $H$  is the magnitude of the uniform field. In superconducting devices it is possible to obtain the  $\beta$  factor as small as part-per-million. This means that it is possible to detect magnetic fields of tens of femtoTesla in a presence of millitesla uniform ambient field.

### 7.3 The Rogowski coil

The special kind of helical coil sensor uniformly wound on a relatively long non-magnetic circular or rectangular strip, usually flexible (Fig. 25) is commonly known as the Rogowski coil, after the description given by Rogowski and Steinhaus in 1912 [4]. Sometimes this coil is called Chattock coil (or Rogowski-Chattock potentiometer, RCP). Indeed, the operating principle of such a coil sensor was as first described by Chattock in 1887 [5] (it is not clear if Rogowski knew the disclosure of Chattock, because in Rogowski's article the Chattock was not cited).

The induced voltage is used as the output signal of the Rogowski coil. But the principle of operation of this sensor is based on the Ampere's law rather than the Faraday's law. If the coil of the length  $l$  is inserted into a magnetic field then the output voltage is the sum of voltages induced in each elementary turn (all turns are connected in series)

$$V = \sum \left( -n \cdot \frac{d}{dl} \cdot \frac{d\phi}{dt} \right) = \mu_0 \cdot \frac{n}{l} \cdot A \cdot \frac{d}{dt} \cdot \int_A^B (H) dl \cdot \cos(\alpha) \quad (30)$$

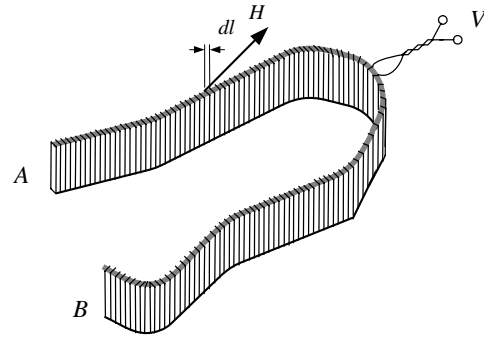


Fig. 25. An example of the Rogowski coil (A, B – ends of the coil)

The output signal of the Rogowski coil depends on the number of turns per unit length  $n/l$  and the cross section area,  $A$ , of the coil. Correctly designed and manufactured Rogowski coil inserted in the magnetic field at fixed points A – B should give the same output signal independently on the shape of the coil between the points A and B. A coil with connected ends (length A-B equal to zero) should have zero output signal.

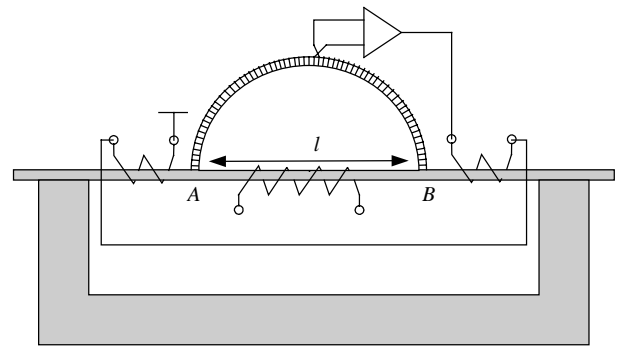


Fig. 26. The application of Rogowski coil for determination of  $H \cdot l$  value

One of the important applications of the Rogowski-Chattock coil is the coil included in the device for testing of magnetic materials – SST device (Single Sheet Tester device) [7,51,52]. In such device it is quite difficult to use the Ampere's law ( $H \cdot l = I \cdot n$ ) for determination of the magnetic field strength  $H$  (from the magnetizing current  $I$ ), because the mean length  $l$  of the magnetic path is not exactly known (in contrary to closed circuit). But if the RCP coil is used we can assume that the output signal of this coil is proportional to the magnetic field strength between the points A-B

$$V = \mu_0 \cdot \frac{n}{l} \cdot A \cdot \frac{d}{dt} (H \cdot l_{AB}) \quad (31)$$

The RCP coil can be used to determine the  $H \cdot l$  value, that is the difference of magnetic potentials. The application of the coil to direct measurements of  $H$  (for fixed value of length  $l_{AB}$ ) is not convenient, because the output signal is relatively small and integration of the output voltage is required. For this reason, the compensation method presented in Fig. 26 is more often used. In such method the output signal of RCP coil is utilized as the signal for the feedback circuit with current exciting the correction coils. Due to the negative feedback circuit the output signal of the coil is equal to zero, which means that

all magnetic field components in the gap air and the yoke are compensated and

$$H \cdot l_{AB} - n \cdot I = 0 \quad (32)$$

Thus, the magnetic field strength can be determined directly from the magnetizing current because the other parameters ( $l_{AB}$  and  $n$ ) are known.

The most important application of the Rogowski coil is for the current measurements [53-57]. When the coil rounds the current conducting wire (Fig. 27) the output signal of the sensor is

$$V = \mu_0 \cdot \frac{n}{l} A \cdot \frac{dI}{dt} \quad (33)$$

The Rogowski coil used as the current sensor enables measurements of very high values of current (including the plasma current measurements in the space [30]). Due to relatively small inductance such sensors can be used to measure transient current of pulse times down to several nanoseconds [57]. Other advantages of the Rogowski coil as the current sensor in comparison with the current transformer are as follows: excellent linearity (lack of the saturating core), no danger of opening of the second winding of current transformer, low cost of preparation. Therefore, the Rogowski current sensor in many applications has practically substituted current transformers. The application of the Rogowski coil for current measurements is so wide that recently Analog Devices equipped the energy transducer (model AD7763) with an integrating circuit for connecting the coil current sensors.

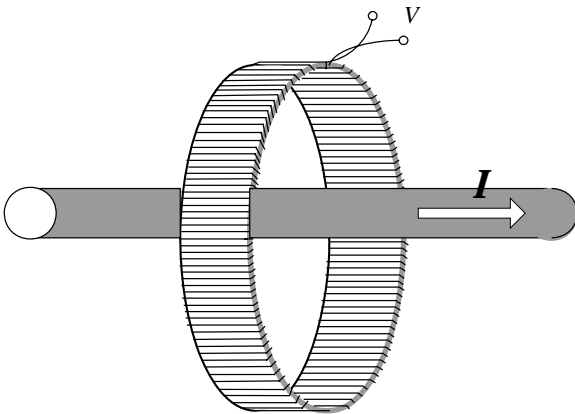


Fig.27. The Rogowski coil as the current  $I$  sensor

Although the Rogowski coil seems to be relative simple in design, careful and accurate preparation is strongly recommended to obtain expected performance [58-60]. First of all, it is important to ensure uniformity of the winding (for perfectly uniform winding the output signal does not depend on the path the coil round the current and on the position of the conductor). Special methods and machines for preparation of the Rogowski coils have been proposed [59-61]. The output signal (thus also the sensitivity) can be increased by the increase of the turn-area, but for correct operation (according to the Ampere's law) it is required to ensure the homogeneity of the flux in each turn. For this reason, the coil is wound on a thin strip with small cross-sectional area. Also, the positioning of the return loop is important – both terminals should be at the same end of the coil. When the coil is wound on a coaxial cable the central conductor can be used as the return path [58].



Fig. 28. An example of the Rogowski coil current sensor – model 8000 of Rocoil [62]

There are several manufacturers offering various types of Rogowski coils or Rogowski coil current sensors. Fig. 28 presents an example of the Rogowski coil transducer (coil and integrator transducer) of Rocoil Rogowski Coils Ltd [62].

#### 7.4. The flux ball sensor

It is quite difficult to manufacture a coil sensor with sufficient sensitivity and small dimensions for measurements of local magnetic fields. If the investigated magnetic field is inhomogeneous, then the sensor averages the magnetic field over the area of the coil. Axially symmetric coil inserted into an inhomogeneous field is insensitive to all even gradients. As it was described in Section 3 for certain coil dimensions ( $l/D \approx 0.67$ ) also the odd gradients can be eliminated.

Brown and Sweer [63] proved that volume average of the field over the interior of any sphere centered at a point is equal to the value of magnetic field at this point. Thus the spherical coil measures the field value at its center. An example of a design of a spherical coil sensor is presented in Fig. 29.

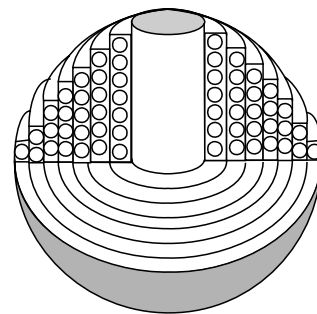


Fig.29. An example of the spherical coil sensor

#### 7.5. Tangential field sensor (H-coil sensor)

Measurements of the magnetic field strength in magnetic materials (for example electrical steel sheet) utilize the fact that the magnetic field inside of the magnetic materials is the same as the tangential field component directly above this material. Thus, a flat coil called H-coil is often used for the measurements of the magnetic field strength [64,65].

The coil sensor for tangential component measurements should be as thin as possible. This is conflicting with the requirement of obtaining sufficient sensitivity of the sensor, which depends on the cross-section area of the coil. A typical coil sensor with thickness 0.5 mm and area 25 mm × 25 mm wound with the wire 0.05 mm in

diameter (about 400 turns) exhibits sensitivity of around  $3 \mu\text{V}/(\text{A}/\text{m})$  [8].

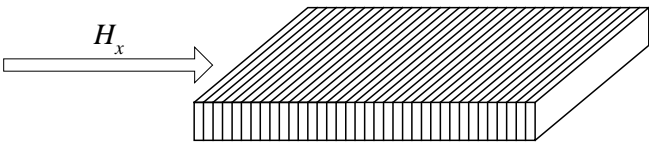


Fig.30. An example of a typical H-coil sensor

In order to obtain sufficient sensitivity the coil sensor is manufactured with the thickness of about 0.5 mm or more. Thus the axis of the coil is distanced from the magnetic material surface. Nakata [66] proposed the use of two-coil system – from two results the value of magnetic field directly at the surface can be extrapolated. This idea was tested numerically and experimentally [8]. It was proved that such method enables the determination of the magnetic field at the magnetic material surface even if the sensor is distanced from this surface more than 1 mm. Additionally it was proposed to enhance the two-coil method by application of up to four parallel (or perpendicular) sensors. The example of such multi-coil sensor is presented in Fig. 31b.

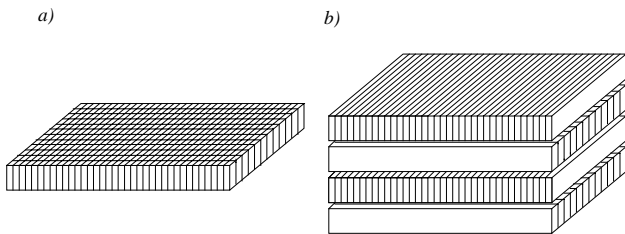


Fig.31. Two examples of a coil sensor for two-components of magnetic field

### 7.6. The needle sensors (B-coil sensors)

When it was necessary to determine the local value of the flux density in electrical steel sheet practically only one method was available (apart from the optical Kerr method): to drill two micro-holes (with diameter  $0.2 \div 0.5 \text{ mm}$ ) and to wind one- or more-turn coil (Fig. 32a).

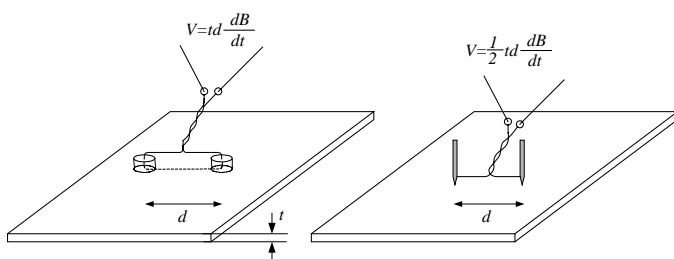


Fig.32. Two methods of local flux density measurements : micro-holes method and needle method

However, drilling of such small holes in relatively hard material is practically not easy. Moreover, this method is destructive. In order to avoid these problems, several years ago Japanese researchers [10,65,66] returned to an old Austrian patent of Werner [9]. Werner proposed to form the one-turn coil by using two pairs of needles, but the application of his invention was difficult, due to relatively small (less than mV) output signal of the sensor. Experimental and theoretical analysis [10,11,65-69] proved that today this method can be

used with satisfying results. It is sufficient to use one pair of needles to form a half-turn coil sensor - the induced voltage is described by the following relation

$$V \approx \frac{1}{2} \cdot t \cdot d \cdot \frac{dB}{dt} \quad (34)$$

where  $t$  is the thickness of the steel sheet and  $d$  is the distance between the needles.

Although the needle method is not as accurate as the micro-holes method, it is widely used for the flux density measurements, especially in two-dimensional testing of electrical steel in form of the sheet. To ensure correct contact with insulated surface of the sample the needle tip should be specially prepared [69].

## 8. COIL SENSOR USED AS A MAGNETIC ANTENNA

The coil sensors, similarly as other magnetic field sensors, often are used for measurements of non-magnetic values. They are used in NDT (Non Destructive Testing), as proximity sensors, current sensors, reading heads etc. But detection of the magnetic field is their primary application, which importance currently increases due the necessity of the stray field investigations (especially for electromagnetic compatibility and protection against dangerous magnetic fields in human environment).

University laboratories are often visited by ordinary people, who live near a transformer station or power transmission lines. They are wondering if such a situation is anyhow dangerous for their health, and they are genuinely interested in measuring the magnetic field intensity.

The advice is simple – *you can do it yourself*. It is sufficient to wind for example 100 turns of a copper wire on a non-magnetic tube (5 to 10 cm diameter) (Fig.1) and to measure the induced voltage. Then, if for instance  $f = 50 \text{ Hz}$ ,  $n = 100$  and  $D = 10 \text{ cm}$  we obtain (according to the relations (7) and (8)) simple expression for output voltage:  $V[\text{V}] \approx 246.5 B [\text{T}]$  or  $V[\text{V}] \approx 0.3096 \cdot 10^{-3} H [\text{A}/\text{m}]$ . Of course, there are many commercially available more or less professional measuring instruments using similar method. Figure 33 presents the limiting exposure to time-varying magnetic fields recommended by ICNIRP (International Commission on Non-Ionizing Radiation Protection) and WHO (World Health Organization) [70].

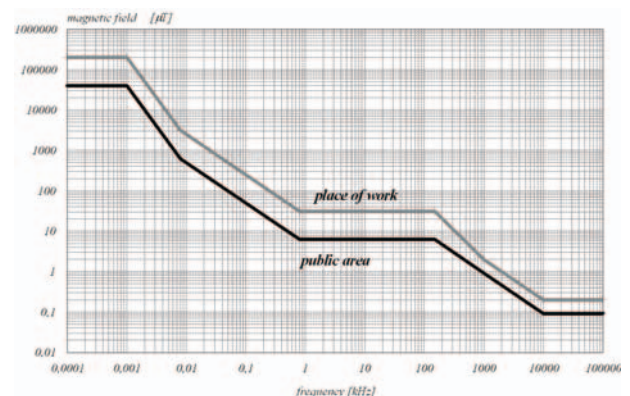


Fig. 33. Reference levels of magnetic field recommended by ICNIRP [70]

Moreover, starting from 2006 all products indicated as CE sign should fulfill European Standard EN 50366:2003 “Household and similar appliances – Electromagnetic Fields – Methods for evaluation and measurements”. Figure 34 presents the professional measuring instrument of Narda [71] designed for determination of

electromagnetic compatibility conditions according to the European Standard EN 50366.



Fig.34. An example of a search coil magnetometer used for testing the electromagnetic compatibility (with permission of Narda Company)

The European Standard EN 50366 requires that magnetic field value should be isotropic. Because the coil sensor detects magnetic field only in one direction, a three-coil system (presented in Fig.3) should be used and then the value of magnetic field should be determined as:

$$b(t) = \sqrt{b_x^2(t) + b_y^2(t) + b_z^2(t)} \quad (35)$$

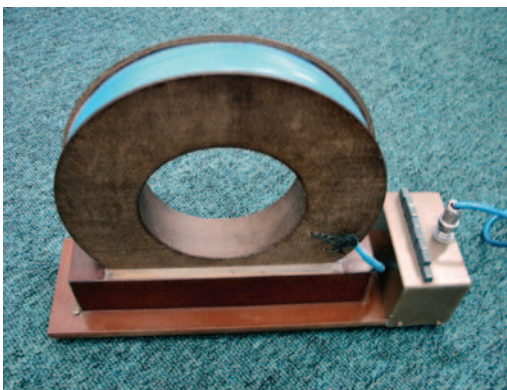


Fig. 35. The air coil sensor designed for investigations of magnetic pollution

For investigations of magnetic pollution (magnetic smog) the author designed and constructed magnetometer consisting of an air coil sensor (Fig. 35) and amplifier/frequency correction system (Fig. 36). The coil was wound onto a ring with diameter 60 mm and width 35 mm using wire 0.1 mm in diameter. The number of turns was 70 000; the coil was divided in seven sections with 10 000 turns each. The frequency characteristics of this sensor are presented in Fig. 36, and the summary of sensor performance in Table 1.

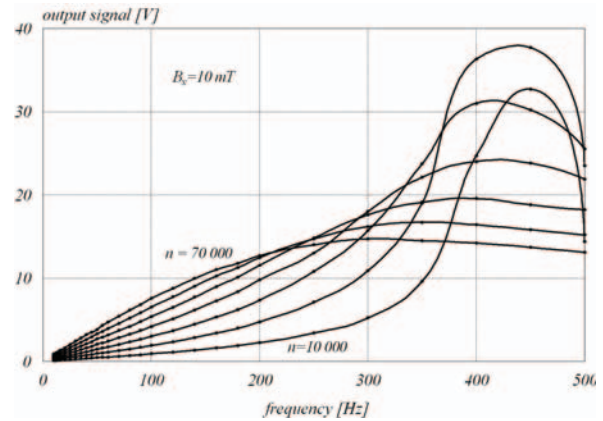


Fig. 36. Frequency characteristics of the constructed sensor

Table 1. Performances of constructed sensor

n	D [mm]	R [kΩ]	L [H]	S/f [mV/μT] for 50 Hz	f <sub>0</sub> [Hz]
10 000	130	8.8	19	45	450
20 000	140	18.2	76	95	430
30 000	147	28.1	168	150	410
40 000	156	38.6	303	210	410
50 000	165	54.1	473	270	380
60 000	173	66	673	330	350
70 000	181	82	932	380	300

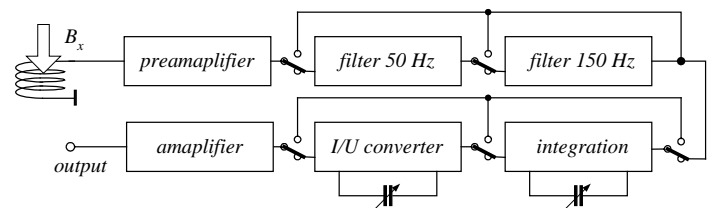


Fig. 37. Block diagram of the induction magnetometer

The block diagram of the constructed magnetometer is presented in Fig. 37. Two filters, 50 Hz and 150 Hz, have been used for elimination of the power frequency components. The tuned integration circuit (for voltage coil input) or current to voltage converter (for current coil input) can be selected by the investigator. Due to large sensitivity of the sensor the smallest attainable range of the magnetometer was 10 pT.

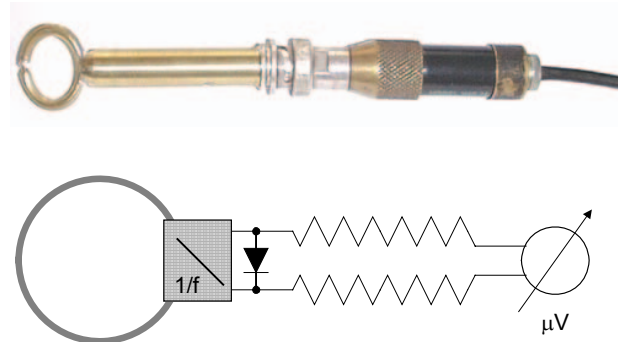


Fig. 38. magnetic field sensor for the frequency bandwidth 0.6 - 2 GHz.

The interest in the measurement of high frequency magnetic fields (up to several GHz) grew with the latest rapid development of high frequency applications, for example mobile phones and their

antennas.. Also in this range of frequency the inductive sensors can be used, although several additional problems appear in this area of application [72]. The dimensions of the sensor should be smaller than the wavelength of the measured field. Therefore, typically measuring instruments are equipped with several sensors. An example of a high frequency field sensor is presented in Fig. 38. Additional problems arise from the fact that in a high frequency electromagnetic field it is rather difficult to separate the electric and magnetic components (especially near the source of the field).



Fig. 39. An induction search coil as a tool for detection of metal objects (with permission of DCG Detector Center)

Coil sensor antenna can be used as pickup coil sensors for detection of metal objects (for example by eddy-current method). An example of such a device is presented in Fig. 39.

Great commercial success can be noted in the application of magnetic antenna in the magnetic article surveillance systems (Fig. 40). Two main types of systems are used.

In the first one [73], thin strips cut from amorphous materials are magnetized by the field emitted from the transmitter antenna. Due to the non-linearity of the magnetic properties the output signal contains harmonics of the predetermined frequency detectable by the receiver antenna.

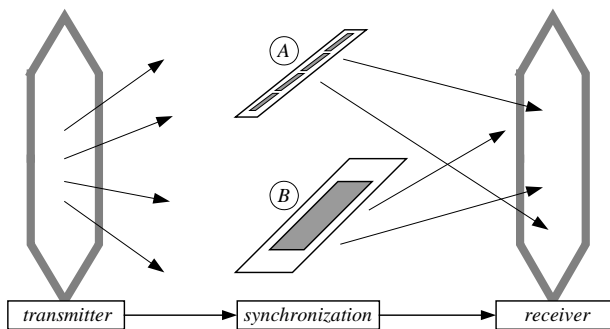


Fig. 40. Magnetic article surveillance system: A) magnetic harmonic system, B) magneto-acoustic system

Currently more efficient magneto-acoustic system was proposed by Herzer [74]. The label is made as a strip made from magnetostrictive amorphous material. Transmitter produces pulses of frequency 58 kHz, 2 ms on and 20 ms off. The vibrating amorphous strip generates signal of frequency 58 kHz, which is detected by the receiving antenna. The system is synchronized, so the antenna is active only during the pause, and therefore the influence of background noise is decreased.

In both systems for the activation or deactivation of the marker is realized by an additional strip made from a semi-hard magnetic material. After demagnetization of this material initially magnetized element, the frequency generated by the label changes and it is not detected by the receiver antenna, thus the deactivation is achieved.

## 9. CONCLUSION

The induction sensors used for the magnetic field measurements (and indirectly other quantities, as for example current) has been known for many years. Today, it is still in common use due to its important advantages: simplicity of operation and design, wide frequency bandwidth and large dynamics.

Due to the simplicity of the transfer function  $V = f(B)$  the performance of the induction coil sensor can be precisely calculated. All factors (number of turns, cross-section area) can be accurately determined and because function  $V = f(B)$  does not include material factors (potentially influenced by external conditions, as for example temperature) the dependence is excellently linear without upper limit (without saturation). The case of core coil sensor is more complicated, because the permeability depends on the magnetic field value and/or temperature. But if the core is correctly designed, then these influences can be significantly reduced.

Due the absence of any magnetic elements and excitation currents the sensor practically does not disturb the measured magnetic field (as compared for instance with the fluxgate sensor).

However, the coil sensors also exhibit some shortcomings. First of all, they are sensitive only to AC magnetic fields, although quasi-static magnetic field (of frequency down to mHz range) can be measured. One notable inconvenience is that the output signal does not depend on the magnetic field value but on the derivative of this field  $dB/dt$  or  $dH/dt$ . Therefore, the output signal is frequency dependent. Moreover, it is necessary to connect an integrating circuit to the sensor, which can introduce additional errors of signal processing.

It is rather difficult to miniaturize the induction coil sensors because their sensitivity depends on the sensor area (or the length of the core). Nevertheless, the micro-coil sensors with dimensions less than 1 mm prepared by using the thin film technology are reported.

Two methods are used for the output electronic circuit: the integrator circuit and the current to voltage transducer. Although digital integration techniques are developed and commonly used, the analogue techniques, especially current to voltage transducers, are often applied due to simplicity and good dynamics.

Certain old inventions, as Chattock-Rogowski coil or needle method are today successfully rediscovered. The importance of the coil sensor also increased recently, because it is easy to measure stray fields generated by electric devices (according to electromagnetic compatibility requirements).

The induction coil sensors with ferromagnetic core prepared from modern amorphous materials exhibit sensitivity comparable to the sensitivity of SQUID sensors. But low magnetic field applications (at pT level) can be still investigated much better by using SQUID methods. On the other hand, for large magnetic fields (above 1 mT) more convenient is to use the Hall sensors.

Also other competitive sensors (flux-gate sensors for field below around 100  $\mu$ T and magnetoresistive sensors for field above around 100  $\mu$ T) are the winners in many applications— especially when the miniaturization is required. For example, a spectacular “defeat” was the substitution of inductive reading heads in the hard drives by magnetoresistive sensors [75].

Nonetheless, examples of modern sensors and applications presented in this paper prove that inductive sensors still play very important role in the measuring technology.

## REFERENCES

1. G. Dehmel, "Magnetic field sensors: Induction coil (search coil) sensors", Chapter 6 in *Sensors – a comprehensive survey*, vol. 5, VCH Publishers, 1989, pp. 205-254
2. P. Ripka, "Induction sensors", Chapter 2 in *Magnetic sensors and magnetometers*, Artech House, 2001, pp. 47-74
3. H. Zijlstra, "Experimental methods in magnetism", North-Holland Publishing, 1967
4. W. Rogowski, W. Steinhaus, "Die Messung der magnetischen Spannung", („The measurements of magnetic potential“). *Arch. für Elektrotechnik*, vol. 1. 1912, pp. 141-150
5. A.P. Chattock, "On a magnetic potentiometer“, *Phil. Magazine*, vol. 24, 1887, pp. 94-96
6. P. Murgatroyd, "Progress with Rogowski coils“, *EMCWA Conf.*, Chicago, 1996, pp. 369-374
7. G.H. Shirkoohi, A.S. Kontopoulos, "Computation of magnetic field in Rogowski-Chattock potentiometer compensated magnetic tester“, *J. Magn. Magn. Mat.*, vol. 133, 1994, pp. 587-590
8. S. Tumanski, "A multi-coil sensor for tangential magnetic field investigations“, *J. Magn. Magn. Mat.*, vol. 242-245, 2002, pp. 1153-1156
9. E. Werner, „Einrichtung zur Messung magnetischer Eigenschaften von Blechen bei Wechselstrom-magnetisierung“, („The device for testing of electrical steel magnetized by AC field“), *Austrian patent*. No. 191015, 1957
10. K. Senda, M. Ishida, K. Sato, M. Komatsubara, T. Yamaguchi, „Localized magnetic properties in grain-oriented silicon steel measured by stylus probe method“, *Tran. IEEE of Japan*, vol. 117-A, 1997, pp. 941-950
11. H. Pfützner, G. Krismanic, „The needle method for induction tests – sources of error“, *IEEE Trans. Magn.*, vol. 40, 2004, pp. 1610-1616
12. R.J. Prance, T.D. Clark, H. Prance, "Compact room-temperature induction magnetometer with superconducting quantum interference level field sensitivity“, *Rev. Sc. Instr.*, vol. 74, 2003, no. 8, pp. 3735-3739
13. W. Richter, "Induction magnetometer for biomagnetic fields“ (Induktionsmagnetometer für biomagnetische Felder), *Exp. Technik der Physik*, vol. 27, 1979, pp.235-243
14. R.F.K. Herzog, O. Tischler, „Measurement of inhomogeneous magnetic fields“, *Rev. Sc. Instr.*, vol. 24, 1953, pp. 1000-1001
15. W.F. Stuart, "Earth's field magnetometry“, *Rep. Prog. Phys.*, vol.35, 1972, pp. 803-881
16. W.H. Campbell, "Induction loop antennas for geomagnetic field variation measurements“, *ESSA Technical Report*, ERL123-ESL6, 1969
17. K.P. Estola, J. Malmivuo, "Air-core induction coil magnetometer design“, *J. Phys. E.*, vol. 15, 1982, pp. 110-1113
18. S.A. Macintyre, "A portable low noise low frequency three-axis search coil magnetometer“, *IEEE Trans. Magn.*, vol. 16, 1980, no. 5, pp. 761-763
19. G. Schilstra, J.H. van Hateren, "Using miniature sensor coils for simultaneous measurement of orientation and position of small, fast-moving animals“, *J. Neuroscience Methods*, v.83, 1998, pp.125-131
20. H.H. Gatzert, E. Andreeva, H. Iswahjudi, „Eddy-current microsensors based on thin-film technology“, *IEEE Trans. Magn.*, vol. 38, 2002, pp. 3368-3370
21. D.J. Sadler, C.H. Ahn, "On-chip eddy current sensor for proximity sensing and crack detection“, *Sensors and Actuators*, vol. A91, 2001, pp. 340-345
22. T. Hirota, T. Siraiwa, K. Hiramoto, M. Ishihara, „Development of micro-coil sensor for measuring magnetic field leakage“, *Jpn. J.Appl. Phys.*, vol. 32, 1993, pp. 3328-3329
23. S.C. Mukhopadhyay, S. Yamada, M. Iwahara, "Experimental determination of optimum coil pitch for a planar mesh-type micromagnetic sensor“, *IEEE Trans. Magn.*, vol. 38, 2002, pp. 3380-3382
24. L. Zhao, J.D. van Wyk, W.G. Odendaal, "Planar embedded pick-up coil sensor for integrated power electronic modules“, *Applied Power Electronics Conference*, vol.2, 2004, pp. 945-951
25. S. Tumanski, "Analiza mozliwosci zastosowania magnetometrow indukcyjnych do pomiaru indukcji slabych pol magnetycznych“ (in Polish), („Analysis of induction coil performances in application for measurement of weak magnetic field“), *Przeglad Elektr.*, vol. 62, 1986, 137-141
26. R.J. Prance, T.D. Clark, H. Prance, "Ultra low noise induction magnetometer for variable temperature operation“, *Sensors and Actuators*, vol. 85, 2000, pp. 361-364
27. H. Ueda, T. Watanabe, "Linearity of ferromagnetic core solenoids used as magnetic sensors“, *J. Geomagn.Geolectr.*, vol. 32, 1980, pp. 285-295
28. K. Hayashi, T. Oguti, T. Watanabe, L.F. Zambresky, "Absolute sensitivity of a high- $\mu$  metal core solenoid as a magnetic sensor“, *J. Geomagn.Geolectr.*, vol. 30, 1978, pp. 619-630
29. N.F. Ness, "Magnetometers for space research“, *Space Science Reviews*, vol. 11, 1970, pp. 459-554
30. V.E. Korepanow, "The modern trends in space electromagnetic instrumentation“, *Adv. Space Res.*, vol. 32, 2003, pp. 401-406
31. V. Korepanov, R. Berkman, "Advanced field magnetometers comparative study“, *Measurement*, vol. 29, 2001, pp. 137-146
32. A.M.A. Frandsen, R.E. Holzer, E. J. Smith, „OGO search coil magnetometer experiments“, *IEEE Trans. Geoscience Electr.*, vol.7, 1969, pp. 61-74
33. Internet: <http://www.meda.com>
34. S. Yabukami, K. Kikuchi, M. Yamaguchi, K.I. Arai, „Magnetic flux sensor principle of microstrip pickup coil“, *IEEE Trans. Magn.*, vol. 33, 1997, pp. 4044-4046
35. M. Yamaguchi, S. Yabukami, K.I. Arai, "Development of multilayer planar flux sensing coil and its application to 1 MHz – 3.5 GHz thin film permeance meter“, *Sensors and Actuators*, vol. 81, 2000, pp. 212-215
36. H. Ueda, T. Watanabe, "Several problems about sensitivity and frequency response of an induction magnetometer“, *Sci. Rep. Tohoku Univ., Ser. 5. Geophysics*, vol. 22, 1975, pp. 107-127
37. G. Clerc, D. Gilbert, "La contre-reaction de flux applique aux bobines a noyau magnetique utilisee pour l'enregistrement des variations rapides du champ magnetique“, („The feedback of magnetic flux used for measurements of magnetic field by means of coil sensor“), *Ann. Geophys.*, vol.20, 1964, pp. 499-502
38. H.J. Micheel, „Induktionsspulen mit induktiver Gegenkopplung als hochauflösende Magnetfeldsonden“, („The coil with inductive feedback used as magnetic field sensor“), *NTZ Archiv*, Vol. 9, 1987, pp. 97-102
39. R. Scholes, "Application of operational amplifiers to magnetic measurements“, *IEEE Trans. Magn.*, vol. 6, 1970, pp. 289-291
40. J.A. Pettinga, J. Siersema, "A polyphase 500 kA current measuring system with Rogowski coils“, *IEE Proc. B.*, vol. 130, 1983, pp. 360-363
41. R.S. Smith, A.P. Annan, "Using an induction coil sensor to indirectly measure the B-field response in the bandwidth of the transient electromagnetic method“, *Geophysics*, vol. 65, 2000, pp. 1489-1494
42. G.D'Antona, E. Carminati, M. Lazzaroni, R. Ottoboni, C. Svelto, „AC current measurements via digital processing of Rogowski coils signal“, *IEEE Instr. and Meas. Technol. Conf.*, Anchorage, 2002, pp. 693-698
43. G.D'Antona, M. Lazzaroni, R. Ottoboni, C. Svelto, „AC current-to-voltage transducer for industrial application“, *IEEE Instr. and Meas. Technol. Conf.*, Vail, 2003, pp. 1185-1190
44. T. Eriksson, J. Blomgren, D. Winkler, „An HTS SQUID picovoltmeter used as preamplifier for Rogowski coil sensor“, *Physica C*, vol. 368, 2002, pp. 130-133
45. J. Groszkowski, "The vibration magnetometer“, *J. Sc. Instr.*, vol.14, 1937, pp. 335-339
46. W. Hagedorn, H.H. Mende, "A method for inductive measurement of magnetic flux density with high geometrical resolution“, *J. of Physics E*, vol. 9, 1976, pp. 44-46
47. R. E. Hetrick, "A vibrating cantilever magnetic field sensor“, *Sensors and Actuators*, vol. 16, 1989, pp. 197-207
48. D. Jiles, "Magnetism and magnetic materials“, *Chapman & Hall*, 1998
49. V. Senaj, G. Guillot, L. Darrasse, "Inductive measurement of magnetic field gradients for magnetic resonance imaging“, *Rev. Sc. Instr.*, vol. 69, 1998, pp. 2400-2405
50. R.L. Fagaly, "Superconducting Quantum Interference Devices“, Chapter 8 in *Magnetic sensors and magnetometers*, Artech House, 2001, pp. 305-347
51. A. Nafalski, A.J. Moses, T. Meydan, M.M. Abousetta, „Loss measurements on amorphous materials using a field-compensated single strip tester“, *IEEE Trans. Magn.*, vol. 25, 1989, pp. 4287-4291
52. A. Khalou, A.J. Moses, T. Meydan, P. Beckley, "A computerized on-line power loss testing system for the steel industry, based on the Rogowski Chattock potentiometer compensation technique, *IEEE Trans. Magn.*, vol. 31, 1995, pp. 3385-3387
53. R.L. Stoll, "Method of measuring alternating currents without disturbing the conducting circuit“, *IEE Proc.*, vol. 122, 1975, pp. 1166-1167
54. D.G. Pellinen, M.S. di Capua, S.E. Sampayan, H. Gerbracht, M. Wang, „Rogowski coil for measuring fast, high-level pulsed currents“, *Rev. Sc. Instr.*, vol. 51, 1980, pp. 1535-1540
55. V. Nassisi, A. Luches, "Rogowski coils: theory and experimental results“, *Rev. Sc. Instr.*, vol. 50, 1979, pp. 900-902
56. D.A. Ward, J. L. T. Exon, "Using Rogowski coils for transient current measurements“, *Eng. Science and Educ. Journal*, 1993, pp. 105-113
57. H. Bellm, A. Küchler, J. Herold, A. Schwab, „Rogowski-Spulen und Magnetfeldsensoren zur Messung transierter Ströme im Nanosekundenbereich“, („The Rogowski coil and magnetic field sensors used for measurements of

- the current pulses in nanosecond range“), Arch. Elektr., vol. 68, 1985, pp. 63-74
58. P.N. Murgatroyd, A.K.Y. Chu, G.K. Richardson, D. West, G.A. Yearley, A.J. Spencer, “Making Rogowski coils”, *Meas. Sci. Technol.*, vol. 2, 1991, pp. 1218-1219
  59. P. Murgatroyd, “Making and using Rogowski coil”, *ICWA Conf.*, Cincinnati, 1992, pp. 267-274
  60. P. Murgatroyd, D.N. Woodland, “Geometrical properties of Rogowski sensors”, *IEE Colloquium on Low Frequency Power Measurement and Analysis*, London, 1994, pp. 901-910
  61. Ramboz J.D., “Machinable Rogowski coil, design and calibration”, *IEEE Trans. Instr. Meas.*, vol. 45, 1996, pp. 511-515
  62. Internet: <http://www.rocoil.co.uk>
  63. F.W. Brown, J.H. Sweer, “The flux ball – a test coil for point measurements of inhomogeneous magnetic field”, *Rev. Sc. Instr.*, vol. 16, 1945, pp. 276-279
  64. H. Pfützner, P. Schönhuber, „On the problem of the field detection for single sheet testers“, *IEEE Trans. Magn.*, vol. 27, 1991, pp. 778-785
  65. T. Nakata, Y. Ishihara, M. Nakaji, T. Todaka, „Comparison between the H-coil method and the magnetizing current method for the single sheet tester“, *J. Magn. Magn. Mat.*, vol. 215-216, 2000, pp. 607-610
  64. T. Nakata, Y. Kawase, M. Nakano, „Improvement of measuring accuracy of magnetic field strength in single sheet testers by using two H-coils“, *IEEE Trans. Magn.*, vol. 23, 1987, pp. 2596-2598
  65. T. Yamaguchi, K. Senda, M. Ishida, K. Sato, A. Honda, T. Yamamoto, “Theoretical analysis of localized magnetic flux measurement by needle probe”, *J. Phys. IV*, vol. 8, 1998, Pr2, pp. 717-720
  66. K. Senda, M. Ishida, K. Sato, M. Komatsubara, T. Yamaguchi, “Localized magnetic properties in grain-oriented electrical steel measured by needle probe method”, *Electr. Eng. in Japan*, vol. 126, 1999, pp. 942-949
  67. G. Loisos, A.J. Moses, „Critical evaluation and limitations of localized flux density measurements in electrical steels“, *IEEE Trans. Magn.*, vol. 37, 2001, pp. 2755-2757
  68. J. Oledzki, S. Tumanski, “Pomiary indukcji magnetycznej w blachach elektrotechnicznych metoda iglowa”, (in Polish), („Measurements of the flux density in electrical steels by means of the needle method”), *Przegl. Elektr.*, vol. 79, 2003, pp. 163-166
  69. G. Krismanic, H. Pfützner, N. Baumgartinger, „A hand-held sensor for analyses of local distribution of magnetic fields and losses”, *J. Magn. Magn. Mat.* vol. 215-216, 2000, pp. 720-722
  70. Guidelines on Limiting to Non-Ionizing Radiation, ICNIRP (International Commission on Non-Ionizing Radiation Protection) and WHO (World Health Organization), July 1999, ISBN 3-9804789-6-3
  71. Internet: <http://www.narda-sts.com>
  72. Grudzinski E., Rozwalka K., “Szerokopasmowe pomiary pola magnetycznego w ochronie srodowiska – stan obecny i kierunki rozwoju”, (in Polish) („A wideband magnetic field measurements in environment protection – state of the art and new trends”), *Przegl. Elektr.*, vol. 80, 2004, pp. 81-88
  73. US Patent 4484184, Amorphous antipilferage marker, 1984
  74. US Patent 58413348, Amorphous magnetostrictive alloy and surveillance system employing same, 1998
  75. S. Tumanski, Thin film magnetoresistive sensors, IOP Publ., 2000